American Mineralogist, Volume 63, pages 531–534, 1978

Magmatic trends on alkali–iron–magnesium diagrams

DANIEL S. BARKER

Department of Geological Sciences
The University of Texas at Austin
Austin, Texas 78712

Abstract

If compositions of minerals, as well as of igneous rocks, are projected onto a triangular diagram with alkalis, iron, and magnesium at the apices, the familiar magmatic trends of iron enrichment and alkali enrichment are seen as the results of two simultaneous processes during fractional crystallization. Increase in Fe/(Fe + Mg) in mafic minerals, concurrent with increase in the proportion of felsic to mafic minerals, produces trends of projected residual liquid compositions, of varied curvature. Although the effects of fractionally removing one or more crystalline phases can be qualitatively assessed, the "lever rule" cannot be applied to projected compositions on the alkali–iron–magnesium diagram. Such projection of rock and mineral compositions can, however, give preliminary guidance for testing quantitative petrogenetic models. AFM diagrams should be used with judgement, and only with other projections.

Compositions of igneous rocks involve so many components that projection into two-dimensional diagrams is needed for comparison and discrimination of rock types and samples. One of the most widely used diagrams is a plot of Na + K, Fe, and Mg, either as atomic proportions or as molecular or weight proportions of $Na_2O + K_2O$, FeO (including Fe_2O_3 recalculated to FeO), and MgO. Such diagrams are variously called AFM, FMA, or MFA. The choice of molecular or weight proportions would matter little if consistently applied. Frequently, however, the molecular or weight basis is not specified on published diagrams. Figure 1 shows the same data plotted both ways. Comparison with published trends can be misleading if the basis is not made clear.

Wright (1974) has presented strong arguments against the use of AFM projections. Although agreeing with his objections, I contend that AFM diagrams contain more information than is usually retrieved from these plots, although some of this information may be misleading unless viewed in wider context. The significance of trends on alkali–iron–magnesium diagrams can be better understood by examining the relations between compositions of rocks and their constituent minerals when projected onto the AFM plane. Quartz and the anorthite component of plagioclase are ignored; alkali feldspars, feldspathoids, and the albite in plagioclase project to the alkali corner. AFM projections of some mafic minerals in igneous rocks are shown in Figure 2. Limits of solid solution are inferred from the compositional ranges of mineral analyses tabulated by Deer *et al.* (1962, 1963).

If a single phase is fractionally removed, the projected composition of the remaining liquid moves directly away from the projected composition of that phase. Also, as in other projection schemes, if the fractionated phase continuously changes composition, projected points that represent successive residual liquid compositions will define a trajectory that curves, the liquid composition at any stage being connected to the composition of the coexisting crystalline phase by a tangent to the trajectory. If two or more phases crystallize simultaneously, the residual liquid follows a trend that is the resultant of the fractionation vectors.

The "lever rule" (*e.g.*, Ehlers, 1972, p. 10), however, is inapplicable, because the AFM components make up disparate proportions of the complete compositions before projection. All phases, solid and liquid, with the sole exception of magnetite, contain

0003–004X/78/0506–0531$02.00

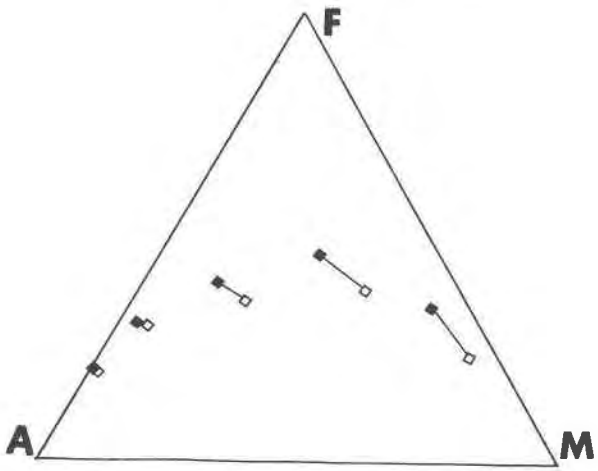

Fig. 1. Whole-rock compositions from the Balcones province, Texas (Spencer, 1969), projected onto AFM. A = $Na_2O + K_2O$, F = FeO + 0.9 Fe_2O_3, M = MgO. Solid symbols indicate weight proportions, unfilled symbols indicate molecular proportions. Lines connect corresponding points for each rock.

other essential components. If SiO_2, TiO_2, Al_2O_3, MnO, CaO, and H_2O are combined at the apex of a tetrahedron with $Na_2O + K_2O$, total Fe as FeO, and MgO as the corners of the base, it is easy to visualize that the phase compositions are at different heights within the tetrahedron, and their relative positions when projected on the base can be grossly misleading. As an example, Figure 3 shows the results of removing 30 weight percent plagioclase of different anorthite contents. The amount of residual liquid migration away from the alkali corner depends not only on the alkali content of the plagioclase but upon the total alkali content of the system. The effect of plagioclase removal is most pronounced in such intermediate rocks as andesite and mugearite, where most of the alkalis reside in plagioclase. Removal of 30 percent plagioclase does not yield a constant ratio of the line segments connecting the alkali corner to initial magma (base of each arrow) and initial magma to residual liquid (tip of each arrow). Thus the lever rule cannot be applied to projected compositions.

In magmatic trends characterized by iron enrichment, increase in Fe/(Fe + Mg) of mafic phases is more rapid than decrease in color index until the mafites are extremely iron-rich, as in the Bushveld Complex (Fig. 4). In the alkali-enrichment trend, decrease in color index is the more rapid; in many examples, even the most mafic, least differentiated rocks have high Fe/(Fe + Mg), as in the Ilimaussaq complex (Fig. 5).

The Bushveld and Ilimaussaq layered intrusions

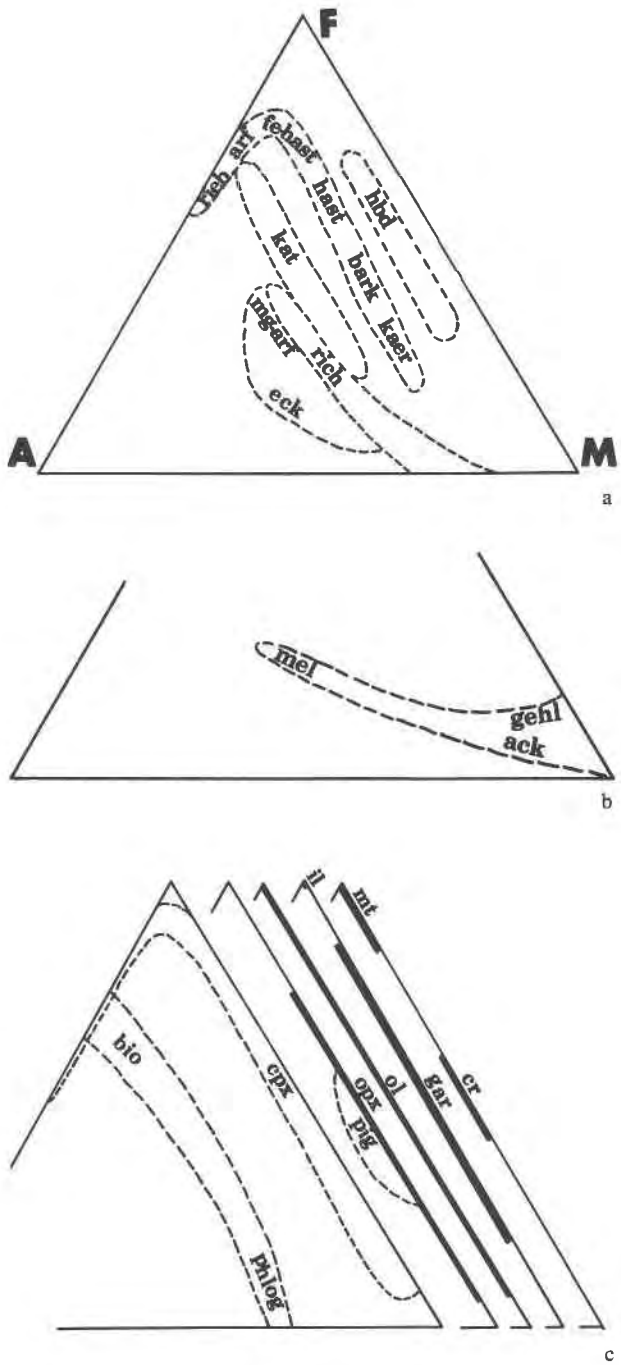

Fig. 2. Igneous mineral compositions, in molecular proportions, projected onto AFM. (a) amphiboles: arf = arfvedsonite, bark = barkevikite, eck = eckermannite, fe-hast = ferrohastingsite, hast = hastingsite, hbd = hornblende, kaer = kaersutite, kat = katophorite, mg-arf = magnesioarfvedsonite, rich = richterite, rieb = riebeckite. (b) melilite series: ack = akermanite, gehl = gehlenite, mel = melilite. (c) bio = biotite, cpx = clinopyroxene, cr = chromite, gar = garnet, il = ilmenite, mt = magnetite, ol = olivine, opx = orthopyroxene, phlog =phlogopite, pig = pigeonite.

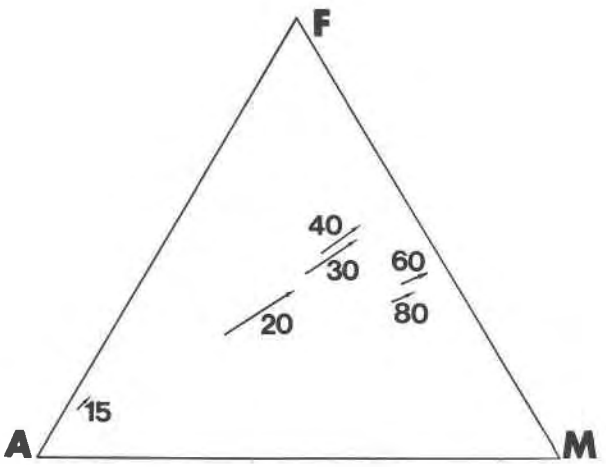

Fig. 3. AFM projection (molecular proportions) showing results of removing 30 weight percent plagioclase of differing anorthite content from several magma compositions. Liquid compositions migrate from the base to the tip of an arrow as plagioclase is removed. Numbers in the diagram refer to weight percent anorthite in the plagioclase. Assumed initial liquids and plagioclase compositions are: basalts, An_{80} and An_{60}; hawaiite, An_{40}; andesite, An_{30}; rhyodacite, An_{20}; rhyolite, An_{15}.

provide examples of crystal fractionation in tholeiitic and strongly alkalic magmas. For the Bushveld rocks, the trend of residual liquids (noncumulus rocks) reflects removal of cumulus olivine, pyroxenes, chromite, and magnetite; scatter is introduced by fractionation of calcic plagioclase. In the earliest stages, orthopyroxene and clinopyroxene control the trend of residual liquids. After maximum iron enrichment is attained, removal of fayalitic olivine, iron-rich clinopyroxene, and magnetite drives the liquid compositions toward the alkali corner. Cumulus rocks contain variable proportions of magnesian cumulus crystals and more alkali-rich intercumulus material, formerly liquid; their compositions lie on lines of mixing, not of fractionation.

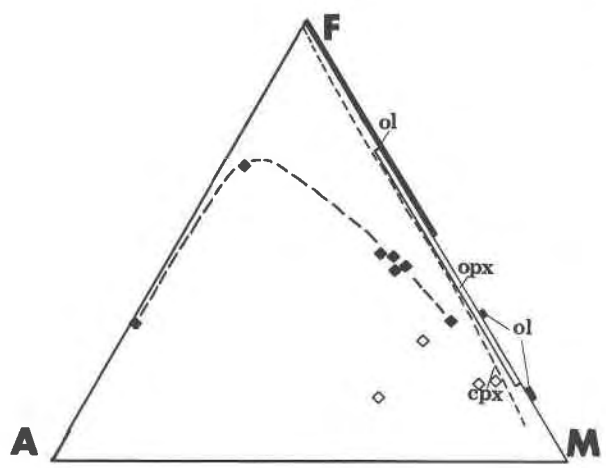

Fig. 4. AFM projection (molecular proportions) of rocks and cumulus minerals, Bushveld Complex, South Africa. Solid symbols represent noncumulus rocks (residual liquids); unfilled symbols represent cumulus rocks. Mineral abbreviations are those in Figure 2. Data are from Frick (1973); Wager and Brown (1967); Daly (1928); Gruenewaldt (1972); Van Zyl (1970); Atkins (1969).

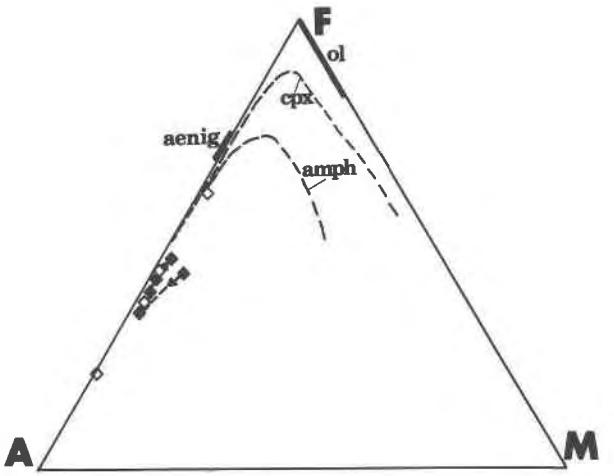

Fig. 5. AFM projection (molecular proportions) of rocks and cumulus minerals, Ilimaussaq Complex, southwest Greenland. Rock symbols as in Figure 4. Aenig = aenigmatite, amph = amphiboles. Other mineral abbreviations are those in Figure 2. Data are from Ferguson (1970); Larsen and Steenfelt (1974); Larsen (1976). Residual liquids evolved toward A, then toward F.

At Ilimaussaq, even the most "primitive" liquid, augite syenite, is salic and low in magnesium, as are the cumulus phases. The sharp reversal of trend for residual liquids, toward alkalis and then toward iron, appears to be characteristic of peralkaline magmas, in which Na-, Fe-rich mafic phases tend to crystallize late. Another alkaline but noncumulus example of the reversed trend appears in Figure 6. In neither example is the late-stage reversal caused by plagioclase fractionation, because plagioclase stopped precipitating very early. Instead, fractional removal of alkali feldspar produced iron-rich peralkaline residual liquid.

Irvine and Baragar (1971, p. 529 and Fig. 2) proposed that tholeiitic and calc–alkaline suites be defined by their trends on AFM diagrams. The projected compositions of tholeiitic rocks show stronger iron enrichment and, commonly, a more tightly clustered and linear array produced by fractionation of mafic phases with approximately constant Fe/(Fe + Mg). In contrast, calc–alkaline suites show greater scatter, probably caused by more pronounced fractionation of plagioclase.

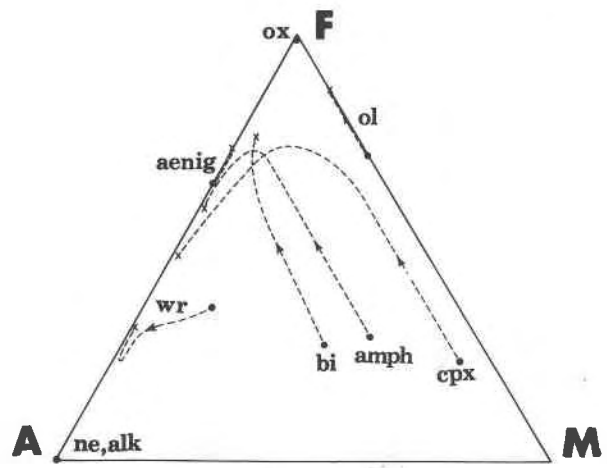

Fig. 6. AFM projection (molecular proportions) of noncumulus rocks and minerals, shallow intrusive bodies in the Diablo Plateau, Texas and New Mexico (Barker *et al.*, 1977). WR = whole rock compositions, NE = nepheline, ALK = alkali feldspar, OX = titanomagnetite. Other mineral abbreviations are those in Figures 2 and 5. Solid dots indicate compositions earliest in the differentiation sequence; ×'s indicate compositions in the latest stages; arrows show directions of compositional change.

With the exception of the oxide–oxide diagram convincingly advocated by Wright (1974), variation diagrams, especially AFM projections, are deceptive to varying degrees. However, if mineral compositions are projected with rock compositions, alkali–iron–magnesium diagrams can be used, in concert with textural and modal data and with other projections, as preliminary tests of fractionation and hybridization models. By comparison of liquid trends with mineral compositions, it is possible to single out those phases for which compositional and modal variations control the trend of liquid compositions. Thus, AFM diagrams provide preliminary guides for the essentially empirical and iterative process of petrologic mixing calculations (Wright and Doherty, 1970).

Acknowledgments

Earlier drafts were reviewed by Douglas Smith and Thomas L. Wright. NSF Grant EAR75-22201 supported this work.

References

Atkins, F. B. (1969) Pyroxenes of the Bushveld Intrusion, South Africa. *J. Petrol., 10,* 222–249.

Barker, D. S., L. E. Long, G. K. Hoops and F. N. Hodges (1977) Petrology and Rb–Sr isotope geochemistry of intrusions in the Diablo Plateau, northern Trans-Pecos magmatic province, Texas and New Mexico. *Bull. Geol. Soc. Am., 88,* 1437–1446.

Daly, R. A. (1928) Bushveld igneous complex of the Transvaal. *Bull. Geol. Soc. Am., 39,* 703–768.

Deer, W. A., R. A. Howie and J. Zussman (1962, 1963) *Rock-forming Minerals* (5 volumes). Longmans, London.

Ehlers, E. G. (1972) *The Interpretation of Geological Phase Diagrams.* Freeman, San Francisco.

Ferguson, J. (1970) The differentiation of agpaitic magmas: the Ilimaussaq intrusion, South Greenland. *Can. Mineral., 10,* 335–349.

Frick, C. (1973) The "Sill Phase" and the "Chill Zone" of the Bushveld igneous complex. *Trans. Geol. Soc. South Africa, 76,* 7–14.

Gruenewaldt, G. von (1972) The origin of the roof-rocks of the Bushveld Complex between Tauteshoogte and Paardekop in the eastern Transvaal. *Trans. Geol. Soc. South Africa, 75,* 121–129.

Irvine, T. N. and W. R. A. Baragar (1971) A guide to the chemical classification of the common volcanic rocks. *Can. J. Earth Sci., 8,* 523–548.

Larsen, L. M. (1976) Clinopyroxenes and coexisting mafic minerals from the alkaline Ilimaussaq intrusion, South Greenland. *J. Petrol., 17,* 258–290.

——— and A. Steenfelt (1974) Alkali loss and retention in an iron-rich peralkaline phonolite dyke from the Gardar province, South Greenland. *Lithos, 7,* 81–90.

Spencer, A. B. (1969) Alkalic igneous rocks of the Balcones province, Texas. *J. Petrol., 10,* 272–306.

Van Zyl, J. P. (1970) The petrology of the Merensky Reef and the associated rocks on Swartklip 988, Rustenburg District. In D. J. L. Visser and G. von Gruenewaldt, Eds., *Symposium on the Bushveld Igneous Complex and other Layered Intrusions,* p. 80–107. *Geol. Soc. South Africa, Spec. Publ. 1.*

Wager, L. R. and G. M. Brown (1967) *Layered Igneous Rocks.* Freeman, San Francisco.

Wright, T. L. (1974) Presentation and interpretation of chemical data for igneous rocks. *Contrib. Mineral. Petrol., 48,* 233–248.

——— and P. C. Doherty (1970) A linear programming and least squares computer method for solving petrologic mixing problems. *Bull. Geol. Soc. Am., 81,* 1995–2008.

Manuscript received, September 12, 1977: accepted for publication, January 5, 1978.